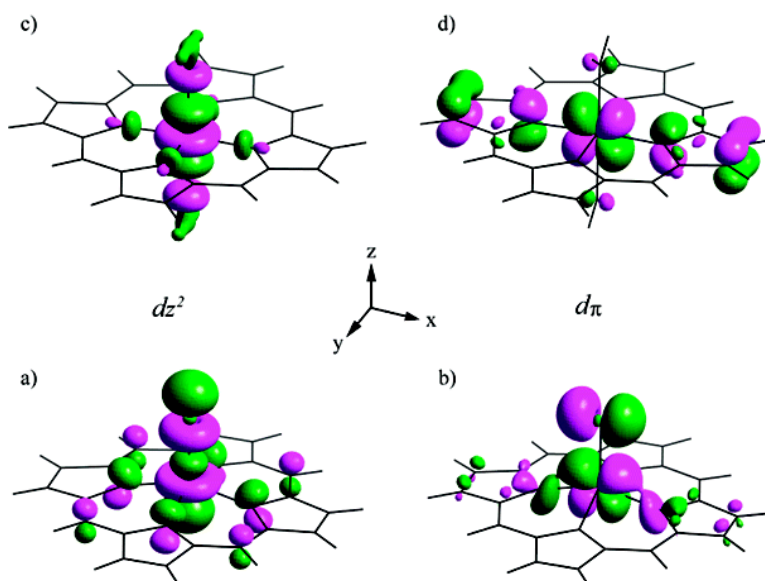Article

Symmetry and Bonding in Metalloporphyrins. A Modern Implementation for the Bonding Analyses of Five- and Six-Coordinate High-Spin Iron(III)–Porphyrin Complexes through Density Functional Calculation and NMR Spectroscopy

Ru-Jen Cheng, Ping-Yu Chen, Timothy Lovell, Tiqing Liu, Louis Noodleman, and David A. Case

More About This Article

Additional resources and features associated with this article are available within the HTML version:

- Supporting Information
- Links to the 7 articles that cite this article, as of the time of this article download
- Access to high resolution figures
- Links to articles and content related to this article
- Copyright permission to reproduce figures and/or text from this article

View the Full Text HTML

Symmetry and Bonding in Metalloporphyrins. A Modern Implementation for the Bonding Analyses of Five- and Six-Coordinate High-Spin Iron(III)−Porphyrin Complexes through Density Functional Calculation and NMR Spectroscopy

Ru-Jen Cheng,*,† Ping-Yu Chen,† Timothy Lovell,‡ Tiqing Liu,‡ Louis Noodleman,‡ and David A. Case‡

Contribution from the Department of Chemistry, National Chung-Hsing University, Taichung, Taiwan 402, Republic of China, and the Department of Molecular Biology, TPC15, The Scripps Research Institute, La Jolla, California 92037

Abstract: Bonding interactions between the iron and the porphyrin macrocycle of five- and six-coordinate high-spin iron(III)−porphyrin complexes are analyzed within the framework of approximate density functional theory with the use of the quantitative energy decomposition scheme in combination with removal of the vacant π^* orbitals of the porphyrin from the valence space. Although the relative extent of the iron−porphyrin interactions can be evaluated qualitatively through the spin population and orbital contribution analyses, the bond strengths corresponding to different symmetry representations can be only approximated quantitatively by the orbital interaction energies. In contrast to previous suggestions, there are only limited Fe → P π^* back-bonding interactions in high-spin iron(III)−porphyrin complexes. It is the symmetry-allowed bonding interaction between d_{z^2} and a_{2u} orbitals that is responsible for the positive π spin densities at the *meso*-carbons of five-coordinate iron(III)−porphyrin complexes. Both five- and six-coordinate complexes show significant P → Fe π donation, which is further enhanced by the movement of the metal toward the in-plane position for six-coordinate complexes. These bonding characteristics correlate very well with the NMR data reported experimentally. The extraordinary bonding interaction between d_{z^2} and a_{2u} orbitals in five-coordinate iron(III)−porphyrin complexes offers a novel symmetry-controlled mechanism for spin transfer between the axial ligand σ system and the porphyrin π system and may be critical to the electron transfer pathways mediated by hemoproteins.

Introduction

The impressively varied biological functions of hemoproteins are mediated by the versatile electronic structures of iron porphyrins. The electronic structures of metalloporphyrins can be controlled by the number and nature of axial ligands and peripheral substituents of the porphyrin macrocycle through bonding interactions between metal and ligands.[1] Many of the transition metal complexes are paramagnetic and have unpaired electrons in metal d orbitals. These unpaired electrons may be transferred to the ligands through different types of metal−ligand bonding interactions, that is, ligand-to-metal σ donation, ligand-to-metal π donation, and metal-to-ligand π back-bonding. Different bonding interactions may result in σ or π spin delocalization and different spin distribution on the ligands. In addition to the variety of oxidation states of iron, the number and spin distribution of these unpaired electrons on the porphyrin

ring or axial ligands may be another mechanism nature chooses to fine-tune the electronic nature of hemoproteins.

Defining x and y axes as lying in the porphyrin plane along trans pyrrole nitrogens and the z axis as perpendicular to the porphyrin plane where axial ligands coordinate, the five d orbitals of central metal will be involved in different types of bonding interactions with porphyrin macrocycle and axial ligands (Figure 1). For four- and six-coordinate metalloporphyrins, with effective symmetry of D_{4h}, the $d_{x^2-y^2}$ orbital interacts with porphyrin σ-type molecular orbitals with nodal planes passing through *meso*-carbons. The d_{z^2} orbital has electron density mainly along the z axis and will interact mostly with axial ligand orbitals of σ symmetry. The metal d_π orbitals (d_{xz} and d_{yz}) may interact with out-of-plane π-type molecular orbitals from the porphyrin macrocycle or axial ligands. The d_{xy} orbital, which points toward the diagonals of the x and y axes, shows weak in-plane π bonding under most circumstances. However, there is recent evidence that for six-coordinate ruffle-shaped metalloporphyrins, the d_{xy} orbital may be involved in the bonding interaction with the a_{2u}-type porphyrin molecular orbital.[2,3] This bonding interaction is a consequence of descend-

*To whom correspondence should be addressed (e-mail rjcheng@ mail.nchu.edu.tw).

† National Chung-Hsing University.

‡ The Scripps Research Institute.

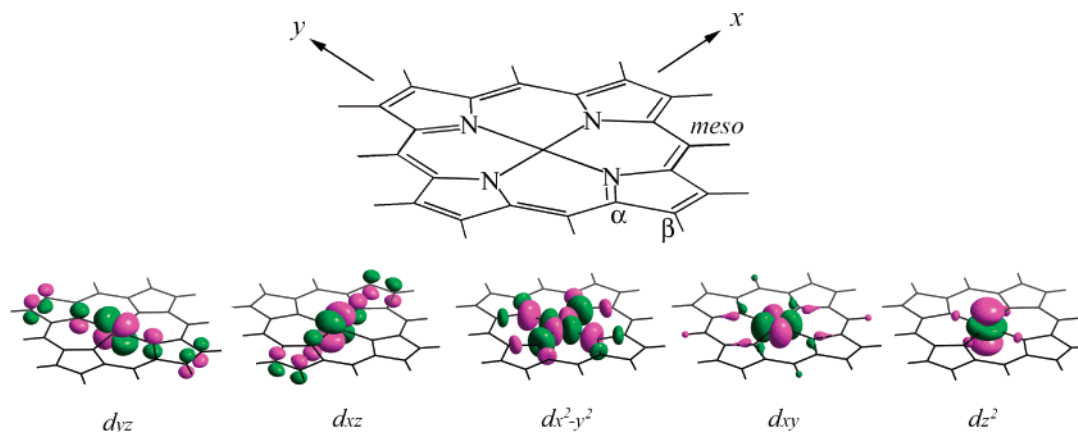(1) Scheidt, W. R.; Reed, C. A. *Chem. Rev.* **1981**, *81*, 543−555.

Figure 1. Atom labeling scheme, coordinate system, and bonding interactions for a four-coordinate metalloporphyrin.

Table 1. Correlation Table for the Molecular Orbitals of Metalloporphyrin[a]

	D_{4h}	D_{2h}	D_{2d}	C_{4v}
metal				
$d_{x^2-y^2}$	b_{1g}	a_g	b_2 (b_1)	b_1
d_{z^2}	a_{1g}	a_g	a_1	a_1
d_{xz}, d_{yz}	e_g	b_{2g}, b_{3g}	e	e
d_{xy}	b_{2g}	b_{1g}	b_1 (b_2)	b_2
porphyrin				
LUMO	e_g	b_{2g}, b_{3g}	e	e
HOMO	a_{1u}	a_u	b_1	a_2
	a_{2u}	b_{1u}	b_2	a_1
HOMO-1	e_g	b_{2g}, b_{3g}	e	e

[a] Symmetry representations for ruffle-shaped deformation are given in the parentheses.

ing symmetry upon porphyrin deformation. Upon ruffling deformation, the symmetry of a six-coordinate metalloporphyrin will be lowered from D_{4h} to D_{2d}; both d_{xy} and a_{2u} will be of b_2 representation and can therefore interact (Table 1). Similar symmetry consideration indicates that for five-coordinate metalloporphyrin with C_{4v} symmetry, both d_{z^2} and a_{2u} will be of the a_1 representation and should be able to interact. The existence of this type of bonding interaction has been suggested rather intuitively by several authors for some metalloporphyrin π-cation radicals with antiferromagnetic coupling.[4-6] In this connection, Ghosh and Trautwein et al. have studied chloroiron corrolates by means of density functional theory (DFT) calculations and proposed that the antiferromagnetic coupling between Fe(III) and π-cation radical results from a symmetry-allowed overlap of the d_{z^2} orbital of the out-of-plane iron with the "a_{2u}-type" orbital of the corrolate ring.[7,8] However, the consequence of this bonding interaction is not generally recognized, especially in the interpretation of NMR spectra of paramagnetic iron porphyrins that are not π-cation radicals.

NMR spectroscopy is a unique technique for the study of the electronic structures of paramagnetic iron porphyrins. Under favorable conditions, it can differentiate between σ and π spin delocalization mechanisms and provide important information about bonding interactions between iron and ligands and the electronic nature of iron–porphyrin complexes.[9-11] Generally, direct spin delocalization from metal to ligand causes positive spin density and downfield shift of the nuclei. Negative spin density corresponding to upfield shift can only be induced from neighboring atoms through indirect spin polarization. Most five-coordinate iron(III)–porphyrin complexes are of high-spin state ($S = {}^5/_2$), and the corresponding NMR spectra have been investigated extensively (Table 2). With all five d orbitals half-filled, unpaired electron density can be transferred through both σ and π bonding skeletons to the porphyrin macrocycle. Whereas both pyrrole-H and pyrrole-α-CH$_2$ are downfield shifted as a consequence of σ spin transfer from the $d_{x^2-y^2}$ orbital, upfield shifted *meso*-H and the reversal in sign of the chemical shifts for *meso*-H and *meso*-α-CH$_2$ are clear indications of positive π spin densities at the *meso*-carbon positions. Because both d_π orbitals (d_{xz} and d_{yz}) are half occupied for high-spin iron(III) complexes, they may be responsible for π spin delocalization. Of the π symmetry frontier orbitals of the porphyrin having proper symmetry to overlap with the d_{xz} and d_{yz} orbitals of the metal, the $e_g(\pi)$ orbitals have nodes at the *meso* positions, whereas the $e_g(\pi^*)$ have large wave function coefficients at the *meso* positions (Figure 2).[12] Therefore, the mechanism of spin delocalization has always been identified as Fe $\rightarrow$ P π^* back-bonding.[9,11,13] However, because an a_{2u}-type π molecular orbital also has large contributions from *meso* positions, these NMR data cannot exclude spin transfer through d_{z^2} and a_{2u} bonding interaction.

Six-coordinate high-spin iron(III)–porphyrin complexes with symmetry higher than D_{2d} should provide a good chance to differentiate these two types of bonding interactions. Whereas the bonding between d_{z^2} and a_{2u} orbitals should disappear, the

(2) Safo, M. K.; Walker, F. A.; Raitsimring, A. M.; Walters, W. P.; Dolata, D. P.; Debrunner, P. G.; Scheidt, W. R. *J. Am. Chem. Soc.* **1994**, *116*, 7760–7770.

(3) Ghosh, A.; Gonzalez, E.; Vangberg, T. *J. Phys. Chem. B* **1999**, *103*, 1363–1367.

(4) Gans, P.; Buisson, G.; Duee, E.; Marchon, J.-C.; Erler, B. S.; Scholz, W. F.; Reed, C. A. *J. Am. Chem. Soc.* **1986**, *108*, 1223–1234.

(5) Erler, B. S.; Scholz, W. F.; Lee, Y. J.; Scheidt, W. R.; Reed, C. A. *J. Am. Chem. Soc.* **1987**, *109*, 2644–2652.

(6) Seth, J.; Palaniappan, V.; Bocian, D. F. *Inorg. Chem.* **1995**, *34*, 2201–2206.

(7) Zakharieva, O.; Schunemann, V.; Gerdan, M.; Licoccia, S.; Cai, S.; Walker, F. A.; Trautwein, A. X. *J. Am. Chem. Soc.* **2002**, *124*, 6636–6648.

(8) Steene, E.; Wondimagegn, T.; Ghosh, A. *J. Phys. Chem. B* **2001**, *105*, 11406–11413.

(9) La Mar, G. N.; Walker, F. A. In *The Porphyrins*, 1st ed.; Dolphin, D., Ed.; Academic Press: New York, 1979; Vol. 4, pp 61–157.

(10) Goff, H. M. In *Iron Porphyrins*, 1st ed.; Lever, A. B. P., Gray, H. B., Eds.; Addison-Wesley Publishing: Reading, MA, 1983; Vol. 1, pp 237–281.

(11) Walker, F. A. In *The Porphyrin Handbook*, 1st ed.; Kadish, K. M., Smith, K. M., Guilard, R., Eds.; Academic Press: San Diego, CA, 2000; Vol. 5, pp 81–183.

(12) Gouterman, M. *J. Mol. Spectrosc.* **1961**, *6*, 138–163.

(13) Goff, H. M.; Shimomura, E. T.; Phillippi, M. A. *Inorg. Chem.* **1983**, *22*, 66–71.

Table 2. NMR Data of Five- and Six-Coordinate Iron(III)−Porphyrin Complexes[a]

complex	spin state	o-H	m-H	p-H	py-H	meso-C	T (°C)	ref
Fe(TPP)Cl	$^5/_2$	∼6	13.5, 12.3	6.4	81.3	500[b]	20	43, 13
Fe(TPP)SO₃CF₃	$^3/_2$, $^5/_2$		12.5	7.49	39.3	418[c]	29	44
Fe(TPP)C(CN)₃	$^3/_2$, $^5/_2$	9.1	12.5	7.59	24.0	396[c]	29	44
Fe(TPP)ClO₄	$^3/_2$, $^5/_2$	9.2	11.9	7.70	13.0	368	29	44, 47
[Fe(TPP)(DMSO)₂]⁺	$^5/_2$	12.4	9.0	9.1	69.7	13[b]	25	this work, 13

complex	spin state	meso-H	CH₂	CH₃	meso-C	T (°C)	ref
Fe(OEP)Cl	$^5/_2$	−54.2	39.6, 43.1	6.64	375	30	10, 45
Fe(OEP)SO₃CF₃	$^3/_2$, $^5/_2$	−24.6	34.6, 49.4	7.2	300	29	44
Fe(OEP)C(CN)₃	$^3/_2$, $^5/_2$	−20.2	40.5, 51.2	7.46		29	44
Fe(OEP)ClO₄	$^3/_2$, $^5/_2$	−5.5	35.5	6.38		29	44
[Fe(OEP)(DMSO)₂]⁺	$^5/_2$	39	46.2	6.2		25	11
Fe(TPrP)Cl	$^5/_2$	(62)[d]	(86.3)[e]			29	46

[a] TPP, dianion of meso-tetraphenylporphyrin; OEP, dianion of octaethylporphyrin; TPrP, dianion of meso-tetrapropylporphyrin. With weaker field axial ligand, five-coordinate complexes show larger contribution from $S = {}^3/_2$. [b] Chemical shifts were reported at 30 °C. [c] Chemical shifts were reported at 26 °C. [d] meso-CH₂. [e] py-H.
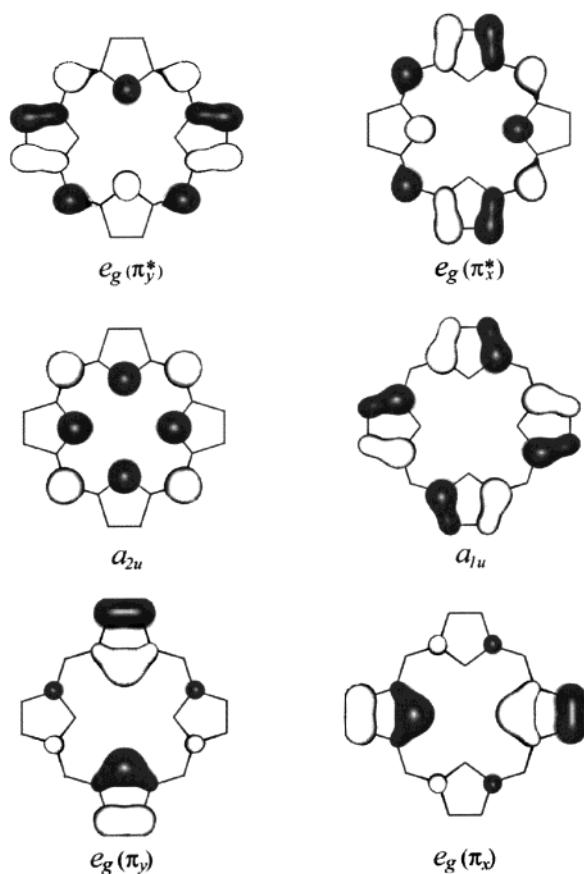
Figure 2. Frontier orbitals of the porphyrin macrocycle.

bonding interactions between d_π and $e_g(\pi^*)$ would be retained and enhanced by the movement of the metal toward the in-plane position for six-coordinate complexes. Upon six-coordination, the NMR chemical shift of the meso-H switches from −54 to 39 ppm and the meso-C shifts from 500 to 13 ppm (Table 2). The reversal in sign for the paramagnetic shifts for both meso-H (relative to the diamagnetic reference of 8.8 ppm) and meso-C (relative to the diamagnetic reference of 121.1 ppm) from five- to six-coordinate high-spin iron(III)−porphyrin complexes suggests negative π spin densities at the meso-carbons and the absence of both bonding interactions in six-coordinate complexes. The most probable source for the negative π spin densities at the meso-carbons is spin polarization from

$e_g(\pi)$ orbitals that may interact with d_π orbitals through P → Fe π donation. However, it is not trivial for iron(III) to switch from a π-base to a π-acid [comparing six- and five-coordinate Fe(III)−porphyrins] just by changing the coordination number. Actually, most experimental evidence supports the porphyrin being a good π-donor in both iron(III) and iron(II) complexes.[14,15] Therefore, the proposition of bonding interactions between d_π and $e_g(\pi^*)$ orbitals in five-coordinate iron(III)−porphyrin complexes needs more sophisticated treatment than just chemical intuition.

A major difference between the populations of a_{2u} and $e_g(\pi^*)$ orbitals is that the $e_g(\pi^*)$ orbitals have much larger contributions from α- and β-carbons than do a_{2u}. However, positive σ spin densities at the α- and β-carbons originating from the $d_{x^2-y^2}$ orbital always dominate the spin transfer pathway and could mask the possible π spin densities at α- and β-carbons of $e_g(\pi^*)$ orbitals for high-spin iron(III) complexes. On the other hand, $e_g(\pi)$ orbitals also have significant contributions from β-carbons. It is almost impossible to differentiate these bonding interactions by paramagnetic NMR analyses alone.

Our previous theoretical studies of five-coordinate iron(III)−porphyrins focused on the bonding interactions that controlled the spin state of the complexes. Careful examination of the molecular orbitals obtained from INDO calculations did reveal bonding interactions between d_{z^2} and a_{2u} orbitals in complexes of C_{4v} symmetry.[16] Higher level molecular orbital calculations may be critical to show the π bonding interactions. Amsterdam Density Functional (ADF)-based calculations have been used to visualize the electron distributions of the low-spin six-coordinate iron(III)−porphyrin complexes and reveal the unusual bonding interaction of d_{xy} and a_{2u} orbitals upon macrocycle ruffling deformation.[3] Very recently, the bonding interactions between d_{z^2} and a_{2u} orbitals have also been realized in high-spin FePCl from similar calculations.[17] To demonstrate the symmetry-controlled nature of this unusual bonding interaction, six-coordinate high-spin iron(III)−porphyrin complexes with symmetry higher than D_{2d} will also be studied as a contrast in this paper. Consistency between the spin population analyses based on theoretical calculations and the experimentally avail-

(14) La Mar, G. N.; Walker, F. A. *J. Am. Chem. Soc.* **1973**, *95*, 1782−1790.
(15) Goff, H. M.; La Mar, G. N.; Reed, C. A. *J. Am. Chem. Soc.* **1977**, *99*, 3641−3646.
(16) Cheng, R.-J.; Chen, P.-Y. *Chem. Eur. J.* **1999**, *5*, 1708−1715.
(17) Ghosh, A.; Vangberg, T.; Gonzalez, E.; Taylor, P. *J. Porphyr. Phthalocyanines* **2001**, *5*, 345−356.

Table 3. Comparison between DFT(BLYP/TZP) Optimized Geometries and Crystal Structural Data for Fe(TPP)Cl and [Fe(TPP)(H₂O)₂]⁺

	Fe(TPP)Cl		[Fe(TPP)(H₂O)₂]⁺		
	calculation	experiment	calculation		experiment
symmetry	C_{4v}		D_{2d}	D_{2h}	
Fe$-$A$_x$	2.214	2.211	2.229	2.236	2.128
Fe$-$N	2.087	2.070	2.036	2.033	2.028
N$-$C$_\alpha$	1.370	1.382	1.376	1.376	1.378
C$_\alpha$$-C_\beta$	1.430	1.432	1.426	1.425	1.437
C$_\alpha$$-C_{meso}$	1.388	1.394	1.394	1.393	1.397
C$_\beta$$-C_\beta$	1.350	1.342	1.358	1.358	1.348
C$_{meso}$$-C_q$	1.486	1.499	1.486	1.486	1.498
Fe$-$C$_{tp}$	0.605	0.59			
Fe$-$C$_{tN}$	0.546	0.49			
ref	this work	25	this work		26

able paramagnetic NMR data will be checked extensively for the first time. Further insight into the orbital interactions and bonding analyses can be accomplished through the available energy decomposition scheme in combination with the appropriate fragment formalism.[18−20] For high-spin iron(III)−porphyrin complexes, energy decomposition analyses will be done with restricted open-shell fragments.[18]

Computational Methods

Density functional calculations have been carried out for high-spin FePCl and [FeP(H₂O)₂]⁺ (P = dianion of porphin) complexes. Full geometry optimizations were done within C_{4v} and D_{2h} symmetry constraints for Fe(TPP)Cl and [Fe(TPP)(H₂O)₂]⁺, respectively. [Fe(TPP)(H₂O)₂]⁺ was also optimized with a D_{2d} symmetry constraint. All calculations reported in this paper are based on the ADF program package characterized by the use of a density fitting procedure to obtain accurate Coulomb and exchange potentials in each SCF cycle, by accurate and efficient numerical integration of the effective one-electron Hamiltonian matrix elements and by the possibility to freeze core orbitals.[21] The molecular orbitals were expanded in an uncontracted triple-ζ STO basis set, augmented with one 2p polarization function for hydrogen; one 3d function for carbon, nitrogen, and oxygen; and one 4p function for iron. The cores (Fe:1s−2p; C, N, O: 1s) have been kept frozen. The LSD exchange correlation potential of Vosko−Wilk−Nusair (VWN) was used in all cases, along with the nonlocal Becke exchange correction[22] and nonlocal Perdew correlation correction.[23] For geometry optimization BLYP exchange correlation correction was the choice. Both spin-restricted and spin-unrestricted formalisms were used as specified for each calculation.

To analyze the iron−porphyrin interaction energies, the energy decomposition scheme developed by Ziegler and Rauk was used.[24,25] The interaction energy between two fragments can be decomposed into three terms:

$$\Delta E_{int} = \Delta E_{elstat} + \Delta E_{Pauli} + \Delta E_{orb}$$

ΔE_{elstat} gives the electrostatic interaction energy between the fragments that is calculated with a frozen electron density distribution in the geometry of the complex. ΔE_{Pauli} gives the repulsive interaction energy between the fragments that is caused by the fact that two electrons with the same spin cannot occupy the same region in space. The term comprises the four-electron destabilizing interactions between occupied orbitals. ΔE_{Pauli} is calculated by enforcing the Kohn−Sham determinant of the whole complex, which is the result of superimposing fragments, to obey the Pauli principle through antisymmetrization and renormalization. The orbital interaction energy, ΔE_{orb}, is a result of the interaction of occupied orbitals on one fragment and vacant orbitals on the other and can be further partitioned into contributions by orbitals that belong to different irreducible representations of the interacting system. To have clear and meaningful energy contributions in the individual

irreducible representations, ionic configurations [P²⁻, high-spin FeCl²⁺, and high-spin Fe(H₂O)₂³⁺] have been used for the energy decomposition analyses.

Results and Discussion

Structural Data. Optimized structures of Fe(TPP)Cl and [Fe(TPP)(H₂O)₂]⁺ with high-spin electronic configuration are compared to available crystallographic data from the Cambridge Structural Database[26] in Table 3. The calculated bond lengths and out-of-plane deviation of iron are in reasonably good agreement with the experimental data for Fe(TPP)Cl.[27] Optimized geometries of [Fe(TPP)(H₂O)₂]⁺ under D_{2d} and D_{2h} symmetry constraints are almost the same other than the orientation of axial ligands, but the calculated bond lengths Fe−A$_x$ are quite different from the experimental results. The D_{2d} symmetry constraint used in [Fe(TPP)(H₂O)₂]⁺ calculation implies that the water molecules are in mutually perpendicular planes of symmetry passed through a pair of opposite pyrrole nitrogens, whereas D_{2h} symmetry implies two parallel water molecules along the same direction. The only crystal structure of [Fe(TPP)(H₂O)₂]⁺ available has a symmetry closer to D_{2h} but with the two water molecules tilted toward different sides.[28] The tilt of the coordinated water may be crucial to the bonding interaction between iron−porphyrin and water.

[Fe(TPP)(H₂O)₂]⁺ has been chosen as a prototype of six-coordinate high-spin complexes including bis(dimethyl sulfoxide) and bis(tetrahydrofuran) iron(III)−porphyrin complexes. Although the orientation of axial ligands may have some effect on the relative stability of the complex, orbital interactions between the two fragments of metal and porphyrin will be mainly mediated by the local symmetry around the iron(III) coordination sphere. It is our purpose to establish the symmetry-

(18) Rosa, A.; Baerends, E. J. *Inorg. Chem.* **1994**, *33*, 584−595.
(19) (a) McGrady, J. E.; Lovell, T.; Stranger, R.; Humphrey, M. G. *Organometallics* **1997**, *16*, 4004−4011. (b) To minimize the effect on the reduction of the size of the basis set, the energy change due to removal of the π* orbital was estimated from the energy difference between the following two calculations. One with all virtual orbitals of *e* symmetry from porphyrin fragment including π* removed. The other one with all virtual orbitals of *e* symmetry from porphyrin fragment but π* removed. (c) It may be ascribed to the same reason as in (b); an attempt to analyze the corresponding spin population changes upon removal of the π* orbital was not successful with the available techniques.
(20) Diefenbach, A.; Bickelhaupt, F. M.; Frenking, G. *J. Am. Chem. Soc.* **2000**, *122*, 6449−6458.
(21) Baerends, E. J.; Ros, P. *Int. J. Quantum. Chem.* **1978**, *S12*, 169−190.
(22) Becke, A. D. *Phys. Rev. A* **1988**, *38*, 3098−3100.
(23) Perdew, J. P. *Phys. Rev. B* **1986**, *33*, 8822−8824.
(24) Ziegler, T.; Rauk, A. *Theor. Chim. Acta* **1977**, *46*, 1.
(25) Ziegler, T.; Rauk, A. *Inorg. Chem.* **1979**, *18*, 1755.
(26) Allen, F. H.; Kennard, O. *Chem. Design Automation News* **1993**, *8*, 31−37.
(27) Scheidt, W. R.; Finnegan, M. G. *Acta Crystallogr.* **1989**, *C45*, 1214−1216.
(28) Cheng, B.; Scheidt, W. R. *Acta Crystallogr.* **1995**, *C51*, 1271−1275.

Table 4. Mulliken Closed-Shell (Open-Shell) Populations for the Iron d Orbitals in FePCl and [FeP(H₂O)₂]⁺ Complexes from Unrestricted DFT Calculations

	$d_{x^2-y^2}$	d_{z^2}	$d_{xz,yz}$	d_{xy}
FePCl	0.3150 (0.6897)	0.3102 (0.6610)	0.1938 (0.8017)	0.0127 (0.9715)
[FeP(H₂O)₂]⁺	0.3522 (0.6637)	0.1605 (0.8362)	0.2074 (0.7797)	0.0186 (0.9635)

controlled bonding interactions in metalloporphyrins. Under D_{2h} symmetry, both $d_{x^2-y^2}$ and d_{z^2} orbitals will be of the same representation and the orbital interaction energies will be mixed together (vide infra). The choice of C_{4v} and D_{2d} symmetries for Fe(TPP)Cl and [Fe(TPP)(H₂O)₂]⁺, respectively, will facilitate the following analyses of orbital interactions between metal and porphyrin. The optimized geometries with hydrogens replacing phenyl substituents at *meso*-positions were used for all of the following calculations.

Orbital Interactions between Iron and Porphyrin. (A) Spin Populations and Orbital Interactions. Table 4 summarizes the calculated closed-shell and open-shell electron populations of the iron *d* orbitals for FePCl and [FeP(H₂O)₂]⁺ complexes. With α and β spin populations $P(\alpha)$ and $P(\beta)$ of each d orbital available from unrestricted calculation, the closed-shell population can be approximated by the number of minority spin or $P(\beta)$ and the open-shell population is equal to the excess of the majority spin or $P(\alpha) - P(\beta)$. For the d⁵ high-spin states, the closed-shell populations of the iron d orbitals represent the electron-density donation from either the axial ligand or the porphyrin, and the open-shell populations are related to the unpaired spin density left over from bonding interactions.[16,29] Generally, increasing closed-shell populations and decreasing open-shell populations indicate increasing bonding interactions between metal and ligands. The results shown in Table 4 indicate that in both FePCl and [FeP(H₂O)₂]⁺ complexes the strongest bonding is the interaction between $d_{x^2-y^2}$ and porphyrin macrocycle, whereas the weakest bonding is the one with d_{xy}. The π-type d orbitals d_{xz} and d_{yz} have significant bonding interactions with ligands. All of these bonding interactions are somewhat stronger in the six-coordinate [FeP(H₂O)₂]⁺ complex. The only interaction that is stronger in the five-coordinate FePCl complex than in the six-coordinate complex is the one with d_{z^2}. This may be ascribed to the strong bonding interaction between d_{z^2} and the axial ligand chloride as shown in Figure 3a and Table 5 (vide infra).

Net charges, gross spin populations, and the corresponding π spin populations of each symmetry-distinct atom type, the porphyrin ring, and the axial ligand for FePCl and [FeP(H₂O)₂]⁺ are collected in Table 5. Net charges and gross spin populations of porphyrin macrocycles suggest that the total bonding interaction between iron and porphyrin for [FeP(H₂O)₂]⁺ is larger than that for FePCl. On the contrary, the bonding interaction with the axial ligand is relatively strong in FePCl. The smaller charge and spin population on iron of FePCl also indicate significant electron donation and spin delocalization between iron and chloride. Detailed analyses of the spin distribution on the macrocycle may disclose specific bonding interactions between iron and porphyrin. The most distinct difference between FePCl and [FeP(H₂O)₂]⁺ is the gross spin populations on the *meso*-carbons, which show opposite signs for five- and six-coordinate complexes. These gross spin populations can be further decon-

(29) Axe, F. U.; Flowers, C.; Loew, G. H.; Waleh, A. *J. Am. Chem. Soc.* **1989**, *111*, 7333−7339.
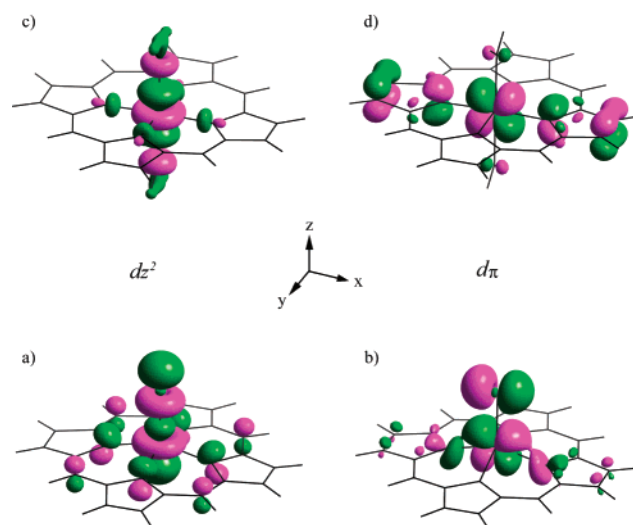
Figure 3. Molecular orbitals based on spin-restricted calculations depicting the bonding interactions between (a) $d_{z^2}-a_{2u}$ and (b) $d\pi-e_g(\pi)$ for five-coordinate C_{4v} FePCl and the corresponding molecular orbitals composed mainly of (c) d_{z^2} and (d) $d\pi$ orbitals for six-coordinate D_{2h} [FeP(H₂O)₂]⁺.

Table 5. Net Charges, (Net Spin Populations), and [the Corresponding π Spin Populations] on Each Symmetry-Distinct Atom Type, Porphyrin, and the Axial Ligand for the High-Spin Iron(III)−Porphyrin Complexes from Unrestricted DFT Calculations

	FePCl	[FeP(H₂O)₂]⁺
Fe	0.7736 (4.0379) [1.5968]	0.9562 (4.1521) [1.5898]
N	−0.4669 (0.0956) [0.0287]	−0.4737 (0.1030) [0.0361]
C_α	0.2649 (0.0015) [−0.0004]	0.2423 (0.0111) [0.0072]
C_β	0.1817 (0.0102) [0.0053]	0.2122 (0.0372) [0.0281]
C_{meso}	0.1080 (0.0228) [0.0174]	0.1701 (−0.0058) [−0.0054]
py-H	−0.2308 (0.0010)	−0.2239 (−0.0012)
meso-H	−0.2037 (−0.0017)	−0.2312 (0.0006)
porphyrin	−0.5232 (0.5684)	−0.2944 (0.7672)
axial ligand	−0.2504 (0.3932)	0.3382 (0.0810)

voluted into the components of π symmetry. Consistent with previous NMR analyses, the *meso*-carbons show positive and negative π spin densities for five- and six-coordinate complexes, respectively. Generally, positive spin densities result from direct spin delocalization through bonds, whereas negative spin densities can be derived only from neighboring atoms through indirect spin polarization. It is noteworthy that almost all of the negative spin populations on the *meso*-carbons of [FeP(H₂O)₂]⁺ are of π symmetry. This is consistent with the spin delocalization into a porphyrin frontier orbital with nodes at the *meso*-carbons or a bonding interaction between d_π and $e_g(\pi)$.

Molecular orbitals involving d_{z^2} and d_π of five- and six-coordinate high-spin iron(III)−porphyrins obtained from spin-restricted ADF calculations are shown in Figure 3. Consistent with previous spin population analyses, the bonding interaction between $d_{x^2-y^2}$ and the nitrogen lone-pairs is most significant, whereas the bonding interaction between d_{xy} and the porphyrin macrocycle is almost invisible in PFeCl (similar to Figure 1).

As we would expect on the basis of symmetry considerations, the bonding interaction between d_{z^2} and a_{2u} orbitals is clearly visible for the five-coordinate complex and not for the six-coordinate complex. On the other hand, the porphyrin-based π molecular orbitals that interact with the metal d_π orbitals are $e_g(\pi)$ instead of $e_g(\pi^*)$ for both five- and six-coordinate complexes. Contrary to previous expectations,[9-11] molecular orbital representations suggest that there is negligible Fe → P π^* back-bonding in five-coordinate iron(III)−porphyrin complexes. Instead, it is the bonding interaction between d_{z^2} and a_{2u} orbitals that should be responsible for the positive π spin densities at the *meso*-carbons.

Due to the concomitance of σ spin transfer mechanism at the β-pyrrole positions, experimental evidence for P → Fe π bonding interactions between metal d_π and $e_g(\pi)$ orbitals is not conclusive in high-spin iron(III)−porphyrin complexes. With weaker field axial ligands, five-coordinate iron(III)−porphyrin complexes have been known to have $S = {}^3/_2$ and ${}^5/_2$ spin state admixture, where a formal spin flip from $d_{x^2-y^2}$ to d_{xy} produces approximately doubly occupied d_{xy} and the σ spin delocalization from the $d_{x^2-y^2}$ orbital will decrease accordingly.[30,31] A pyrrole-H shift from $\sim$80 ppm for $S = {}^5/_2$ complexes toward an extreme of ~ -60 ppm for nearly pure $S = {}^3/_2$ spin state is a clear indication of positive π spin densities at β-pyrrole positions and has been used as a sensitive indicator of the degree of $S = {}^3/_2$ and ${}^5/_2$ spin state admixture.[32,33]

As we would expect by the movement of the metal toward the in-plane position, theoretical calculations show that other than the enhanced σ bonding interaction, P → Fe π bonding interactions between metal d_π and $e_g(\pi)$ orbitals increase even more for six-coordinate complexes as depicted in Figure 3d,b and Table 5. It is interesting to notice that the pyrrole-H shift is smaller and the pyrrole-CH$_2$ shift larger in the six- than in the five-coordinate complexes.[34] This behavior suggests much larger π spin densities at the β-pyrrole positions of the six- than the five-coordinate complexes and supports the conclusion that P → Fe π bonding interactions between metal d_π and $e_g(\pi)$ orbitals are more important in six- than in five-coordinate complexes. The domination of π spin transfer to the β-pyrrole positions for six-coordinate complexes results in a negative net spin population at the corresponding pyrrole-H and makes direct correlation between the calculated spin population and the paramagnetic shift awkward. For high-spin iron(III)−porphyrin complexes, spin delocalization through σ bonding interaction with $d_{x^2-y^2}$ will dominate the whole spin population mechanism. The *meso*-C, located at the nodes of this σ bonding system, happens to be the only site that is insulated from direct σ spin delocalization. This unique nature makes direct correlation with NMR data possible only at the *meso*-C and -H. Further quantitative correlation between the theoretical calculations and

the NMR spectra will be feasible with the evaluation of the unpaired electron spin density on the nuclei[35,36] and the contact shift, as shown in Table S1 and Figure S1 of the Supporting Information for Fe^{III}PCl (P = TPP and OEP). The nice linear relationship demonstrates the promising potential of the theoretical approaches to NMR studies of paramagnetic complexes and further supports previous procedures to dissect the paramagnetic shifts into individual contributions. However, it is not always an easy task to isolate the contact term from the paramagnetic shift.[37,38] In the present work we shall concentrate our attention on the bonding analyses and the consequent spin populations instead of the rather involved contact shift analyses. Correlation between calculated nuclear spin densities and experimental contact shifts has been proved to be applicable to other paramagnetic iron−porphyrins and can be used as a novel approach to the electronic structure of intermediate-spin iron-(II)−porphyrins.[39]

(B) Orbital Contribution Analyses and Spin Polarization. To demonstrate the bonding interaction between metal and porphyrin it is instructive to look at the composition of the individual orbitals. The composition of the representative orbitals in terms of metal and porphyrin fragment orbitals from restricted calculations is given in Table 6. We mainly focus on the molecular orbitals with contributions from the five d orbitals of the metal fragment and the π-type frontier orbitals of the porphyrin fragment (Figure 2). In FePCl, 7b$_2$, 5a$_2$, and 18e orbitals composed of >95% of d_{xy}, a_{1u}, and π^*, respectively, are nonbonding in nature. Similarly, 12b$_2$ and 19e orbitals composed mainly of a_{2u} and π^*, respectively, are nonbonding in [FeP(H$_2$O)$_2$]$^+$. Although a_{2u} has no interaction with the metal in the six-coordinate complex and a_{1u} is nonbonding in the five-coordinate complex, the porphyrin π^* has almost no bonding interaction with the metal in both six- and five-coordinate complexes. Molecular orbitals with contributions from both metal and porphyrin fragments suggest that there are significant interactions between the two fragment orbitals. On the basis of the donor/acceptor nature of porphyrin and metal, orbitals with >50% contribution from the porphyrin fragment are bonding orbitals, and orbitals with >50% contribution from the metal fragment should be antibonding orbitals. These can be further supported by orbital overlaps between porphyrin and metal fragments <Fe^{3+}| P^{2-}> shown in the last column in Table 6. To a first-order approximation, positive overlap indicates bonding and negative overlap correlates to antibonding interaction. On the other hand, the magnitude of the orbital overlap should correspond to the strength of the orbital interaction, which has taken into account the effective orbital overlap in space[20] (Table 7) other than the symmetry and the relative energy considerations. It is important to note that the percent contribution related mainly to the energy match of the fragment orbitals does not always parallel the strength of the bonding interaction. In [FeP(H$_2$O)$_2$]$^+$, the molecular orbital 6b$_1$, with significant

(30) Reed, C. A.; Mashiko, T.; Bentley, S. P.; Kastner, M. E.; Scheidt, W. R.; Spartalian, K.; Lang, G. *J. Am. Chem. Soc.* **1979**, *101*, 2948−2958.
(31) Goff, H.; Shimomura, E. *J. Am. Chem. Soc.* **1980**, *102*, 31−37.
(32) Reed, C. A.; Guiset, F. *J. Am. Chem. Soc.* **1996**, *118*, 3281−3282.
(33) Evans, D. R.; Reed, C. A. *J. Am. Chem. Soc.* **2000**, *122*, 4660−4667.
(34) (a) Budd, D. L.; La Mar, G. N.; Langry, K. C.; Smith, K. M.; Nayyir-Mazhir, R. *J. Am. Chem. Soc.* **1979**, *101*, 6091−6096. (b) On the basis of the characteristic bonding interactions demonstrated in this work, the unusually downfield shifted *py*-H for [Fe(TPP)F$_2$]$^-$ (85 ppm)$^{(c)}$ can only be ascribed to the domination of σ bonding interactions due to the special effect from F$^-$. This rationalization has been confirmed by preliminary calculation for [FePF$_2$]$^+$ with net spin population of (0.0056) and π spin population of [0.0013] at C$_\beta$. More ^{1}H and ^{13}C NMR data for [Fe(TPP)F$_2$]$^-$ and [Fe(OEP)F$_2$]$^-$ complexes are necessary for further bonding analyses. (c) Hickman, D. L.; Goff, H. M. *Inorg. Chem.* **1983**, *22*, 2787−2789.

(35) Wilkens, S. J.; Xia, B.; Weinhold, F.; Markley, J. L.; Westler, W. M. *J. Am. Chem. Soc.* **1998**, *120*, 4806−4814.
(36) (a) Mao, J.; Zhang, Y.; Oldfield, E. *J. Am. Chem. Soc.* **2002**, *124*, 13911−13920. (b) Szterenberg, L.; Latos-Grazynski, L.; Wojaczynski, J. *ChemPhysChem* **2002**, *3*, 575−583.
(37) La Mar, G. N.; Eaton, G. R.; Holm, R. H.; Walker, F. A. *J. Am. Chem. Soc.* **1973**, *95*, 63−75.
(38) Mispelter, J.; Momenteau, M.; Lhoste, J.-M. *J. Chem. Soc., Dalton Trans.* **1981**, 1729−1734.
(39) (a) This work has been presented in ICPP-2, S-139, Kyoto, Japan. (b) Cheng, R.-J.; Chen, P.-Y.; Lin, J.-F.; Liu, T.; Noodleman, L.; Case, D. A. In preparation.

Table 6. Percent Contribution and the Orbital Overlap of P and Iron Fragments to Selected Orbitals (Based on Mulliken Population Analysis per MO) of FePCl and [FeP(H$_2$O)$_2$]$^+$, Where Only the Main Contributions to Each Orbital Have Been Given

FePCl	E (eV)	FeCl^{2+}	P^{2-}	$<$FeCl^{2+} | P$^{2-}>$
18e	−3.10		95.6 (15e−π^*)	−0.005
9b$_1$	−3.20	61.1 (d$_{x^2-y^2}$)	36.3 (8b$_1$)	−0.130
15a$_1$	−3.96	66.6 (d$_{z^2}$)	21.8 (10a$_1$−a$_{2u}$)	−0.066
17e	−4.78	82.4 (d$_{xz}$, d$_{yz}$)	7.8, 6.8 (14e, 13e)	−0.021
5a$_2$	−5.30		99.5 (5a$_2$−a$_{1u}$)	0.000
14a$_1$	−5.40	12.0 (d$_{z^2}$)	65.2, 18.4 (10a$_1$, 8a$_1$)	0.015
7b$_2$	−5.68	95.4 (d$_{xy}$)	2.4 (5b$_2$)	−0.011
16e	−6.20	27.0 (d$_{xz}$, d$_{yz}$)	68.8 (13e−π)	−0.021
7b$_1$	−8.42	28.0 (d$_{x^2-y^2}$)	46.2, 19.3 (8b$_1$, 6b$_1$)	0.048

[FeP(H$_2$O)$_2$]$^+$	E (eV)	Fe(H$_2$O)$_2$$^{3+}$	P^{2-}	$<$Fe(H$_2$O)$_2$$^{3+}$ | P$^{2-}>$
13b$_2$	−5.47	63.3 (d$_{x^2-y^2}$)	35.7 (9b$_2$)	−0.147
19e	−6.07		95.1 (15e−π^*)	−0.008
13a$_1$	−7.26	80.2 (d$_{z^2}$)	9.1 (8a$_1$)	−0.046
12b$_2$	−8.13		82.8, 8.9, 5.8 (8b$_2$−a$_{2u}$, 7b$_2$, 9b$_2$)	−0.002
18e	−8.13	70.2 (d$_{xz}$, d$_{yz}$)	28.3 (13e−π)	−0.031
7b$_1$	−8.31	71.0(d$_{xy}$)	25.0 (6b$_1$−a$_{1u}$)	−0.010
6b$_1$	−8.37	23.7 (d$_{xy}$)	74.4 (6b$_1$−a$_{1u}$)	−0.002
17e	−9.53	26.3 (d$_{xz}$, d$_{yz}$)	60.4 (13e−π)	0.017
10b$_2$	−11.48	26.6 (d$_{x^2-y^2}$)	43.4, 20.1 (9b$_2$, 6b$_2$)	0.051
11a$_1$	−12.26	16.9 (d$_{z^2}$)	69.7 (8a$_1$)	0.012

Table 7. Orbital Overlaps between the Two Fragment Orbitals of Iron and Porphyrin

	orbital overlap $<$[FeCl]$^{2+}$ | P$^{2-}>$				
	$<$1b$_1$(d$_{x^2-y^2}$)\|8b$_1$>	$<$5a$_1$ (d$_{z^2}$)|10a$_1$>	$<$3e (d$_{xz}$)|13e>	$<$3e (d$_{yz}$)|13e>	$<$1b$_2$ (d$_{xy}$)|5b$_2$>
FePCl	0.184	0.081	0.068	0.068	0.048

	orbital overlap $<$[Fe(H$_2$O)$_2$]$^{3+}$ | P$^{2-}>$				
	$<$4b$_2$ (d$_{x^2-y^2}$) | 9b$_2$>	$<$4a$_1$ (d$_{z^2}$) | 8a$_1$>	$<$3e, 4e (d$_{xz}$) | 13e>	$<$3e, 4e (d$_{yz}$) | 13e>	$<$1b$_1$ (d$_{xy}$) | 6b$_1$>
[FeP(H$_2$O)$_2$]$^+$	0.194	0.054	0.087	0.087	0.002

contributions from d$_{xy}$ and a$_{1u}$ (23.7 and 74.4%, respectively), shows very little orbital overlap (−0.002) between the two fragments. This can be ascribed to the very small orbital overlap ($<$1b$_1$ (d$_{xy}$) \| 6b$_1$> = 0.002) between these two fragment orbitals d$_{xy}$ and a$_{1u}$. Other than some minor exceptions resulting from more complicated orbital contributions, the data of orbital overlaps clearly indicate that the bonding interaction with the porphyrin ring is strongest for d$_{x^2-y^2}$ and weakest for d$_{xy}$, consistent with previous spin population analyses.

Although it is instructive to analyze the orbital interactions from spin-restricted calculations, spin-unrestricted calculations with different orbitals for different spins provide a more extensive way to interpret the differential positive and negative spin densities measured in paramagnetic metalloporphyrin complexes.[40,41] Correlations of spin-restricted and -unrestricted one-electron energies for FePCl and [FeP(H$_2$O)$_2$]$^+$ complexes are shown in Figure 4 (left and right sides, respectively). Because the spin density is predominantly located on the iron atom, exchange forces split the iron d levels up to 4 eV, reflecting the favorable exchange interactions among the α spin electrons compared to those of β spin. For high-spin d^5 iron-(III) complexes in which there is more spin density on the iron atom, the exchange splitting of the d orbitals is always larger. Consistent with previous bonding analyses, among the five half-filled d orbitals, the exchange splitting is largest for the most

localized d$_{xy}$ orbital and smallest for the highly delocalized d$_{z^2}$ in FePCl due to axial ligand interaction. There is little spin density on the porphyrin, so that the splitting between spin-up and spin-down orbitals localized on the macrocycle is very small; in the figure, only one line is used to represent both energies.

Another important difference between the spin-restricted and -unrestricted results lies in the percent contribution of the iron d orbitals. Because the spin-up and spin-down orbitals have such different energies, they may interact with the ligand in different fashions. As shown in Figure 4, the orbital shifts are also accompanied by significant changes of the amount of ligand mixing in the molecular orbitals. For the half-occupied d orbitals, the lower-lying spin-up orbitals tend to mix favorably with the ligand orbitals of the same symmetry, indicating significant spin delocalization to the porphyrin macrocycle for α spin. Such interactions are less favorable for the higher energy spin-down orbitals, because the energy mismatch with the ligand orbitals of appropriate symmetry is greater. This type of differential up and down spin delocalization for fully occupied molecular orbitals results in a spin population that is indicative of a spin polarization effect.[40]

(C) Energy Decomposition and Bonding Analyses. Both the spin populations and the orbital contributions are qualitative indications for the relative strengths of the iron−porphyrin interactions but not a quantitative measure of the corresponding energies. Orbital interaction energies can be calculated explicitly according to the energy decomposition scheme.[18] Table 8 shows the results of the partitioning of the interaction energies, ΔE_{int},

(40) Case, D. A. In *Porphyrins: Excited States and Dynamics*; Gouterman, M., Rentzepis, P. M., Straub, K. D., Eds.; American Chemical Society: Washington, DC, 1986; pp 59−71.
(41) Sontum, S. F.; Case, D. A.; Karplus, M. *J. Chem. Phys.* **1983**, *79*, 2881−2892.
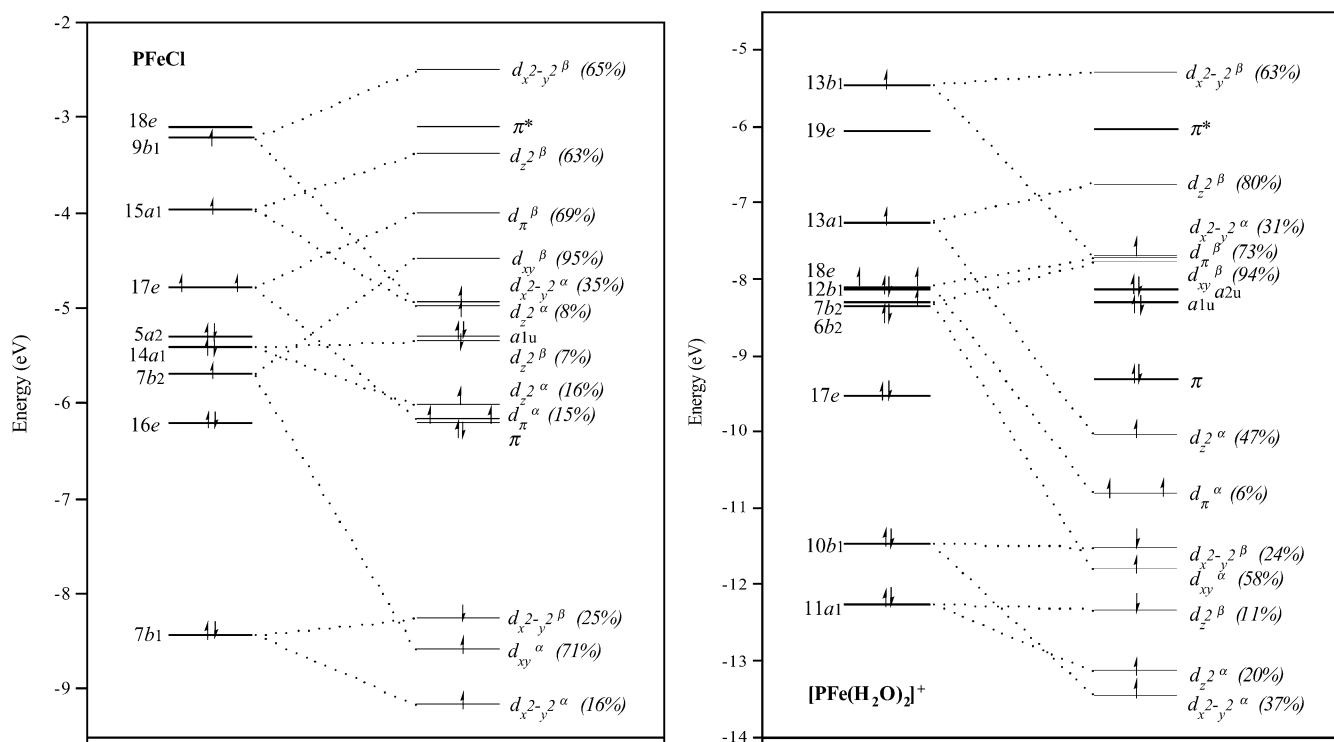
Figure 4. Orbital energies from spin-restricted (left) and spin-unrestricted (right) calculations for FePCl and [FeP(H$_2$O)$_2$]$^+$. In the spin-unrestricted calculations, the small splittings of porphyrin α and β orbitals are not shown. The orbital population is also given for spin-up and spin-down components.

Table 8. Decomposition of the Interaction Energy (Kilocalories per Mole) between the Two Fragments Iron and Porphyrin

		ΔE_{int}	ΔE_{elstat}	ΔE_{Pauli}	ΔE_{orb}	a$_1$ (d$_{z^2}$)	a$_2$	b$_1$ (d$_{x^2-y^2}$)	b$_2$ (d$_{xy}$)	e (d$_{xz}$, d$_{yz}$)
FePCl	all orbitals	−808.91	−574.05	226.35	−461.22	−109.99	−8.46	−112.70	−41.57	−188.50
	remove π^{*a}	10.65	0.00	0.00	10.65	−1.66	−1.16	−2.94	−1.00	17.41

		ΔE_{int}	ΔE_{elstat}	ΔE_{Pauli}	ΔE_{orb}	a$_1$ (d$_{z^2}$)	a$_2$	b$_2$ (d$_{x^2-y^2}$)	b$_1$ (d$_{xy}$)	e (d$_{xz}$, d$_{yz}$)
[FeP(H$_2$O)$_2$]$^+$	all orbitals	−1071.52	−754.67	262.93	−579.77	−117.13	−9.53	−141.73	−51.28	−260.11
	remove π^{*a}	12.19	0.00	0.00	12.19	−1.98	−0.80	−8.41	0.30	23.08

^{a} Estimation of the energy change due to removal of the π^* orbital.[17b]

between iron ([Fe−Cl]$^{2+}$ or [Fe(H$_2$O)$_2$]$^{3+}$]) and porphyrin (P^{2-}) fragments into the three terms, ΔE_{elstat}, ΔE_{Pauli}, and ΔE_{orb}. The electrostatic interaction energy ΔE_{elstat} is highly stabilized due to the large attractive interaction between the charged fragments and is stabilized even more for [FeP(H$_2$O)$_2$]$^+$ with the tripositive cation [Fe(H$_2$O)$_2$]$^{3+}$. The Pauli repulsion ΔE_{Pauli}, arising from the two-orbital four- or three-electron destabilizing interactions between occupied orbitals on the two fragments, is larger for [FeP(H$_2$O)$_2$]$^+$ due to the larger number of closed-shell electrons in [Fe(H$_2$O)$_2$]$^{3+}$. Stabilization through orbital interactions is depicted by ΔE_{orb} and is more effective for [FeP(H$_2$O)$_2$]$^+$.

Table 8 also gives the contributions of the stabilizing orbital interaction term for the orbitals with different symmetry. Due to the fact that in high-spin iron(III) complexes all of the bonding interactions between metal d and porphyrin orbitals are two-orbital three-electron interactions, that is, the corresponding antibonding orbital is occupied by one electron, orbital interaction energies involving metal d orbitals would be even larger without this destabilization.[18] Consistent with previous analyses, the energy term $\Delta E(d_{x^2-y^2})$ that accounts for nitrogen lone-pair in-plane σ donation into the metal d$_{x^2-y^2}$ orbital is largest for both five- and six-coordinate complexes. The contribution of the $\Delta E(d_{xy})$ term is small but not negligible. The bonding interaction decreases in the same order d$_{x^2-y^2}$ > d$_{z^2}$, d$_{xz,yz}$ > d$_{xy}$

for both systems in line with the orbital overlap shown in Table 6. As expected, the in-plane σ bonding and out-of-plane π bonding are stronger when the metal is sitting in the plane of the macrocycle in the six-coordinate [FeP(H$_2$O)$_2$]$^+$ complex (vide infra).

Contrary to previous orbital contribution and orbital overlap analyses, the bonding interaction energy $\Delta E(d_{z^2})$ is somewhat larger for [FeP(H$_2$O)$_2$]$^+$. This could be rationalized by the nature of the bond. Althought the bonding interaction between d$_{z^2}$ and a$_{2u}$(10a$_1$) in FePCl is of π type (as depicted in Figure 3a), that between d$_{z^2}$ and nitrogen lone-pair 8a$_1$ in [FeP(H$_2$O)$_2$]$^+$ is of σ type. It is reasonable that the stabilizing contribution arising from the σ bond is larger than that from the π bond. Even though the orbital overlaps between the two fragment orbitals (<5a$_1$ - (d$_{z^2}$) | 10a$_1$> = 0.081 and <4a$_1$ (d$_{z^2}$) | 8a$_1$> = 0.054) shown in Table 7 also favor the bonding interaction of d$_{z^2}$ in FePCl, it must be the spatial distribution of the electron density that contributes to the strength of the σ bond.

We have tried to extract and rationalize all useful information from the calculation. All of the qualitative and quantitative analyses up to this point seem to correlate very well. To avoid pushing the data too far, one important point that has to be addressed very carefully is that the contributions of the orbital interactions ΔE_{orb} do not come only from genuine orbital
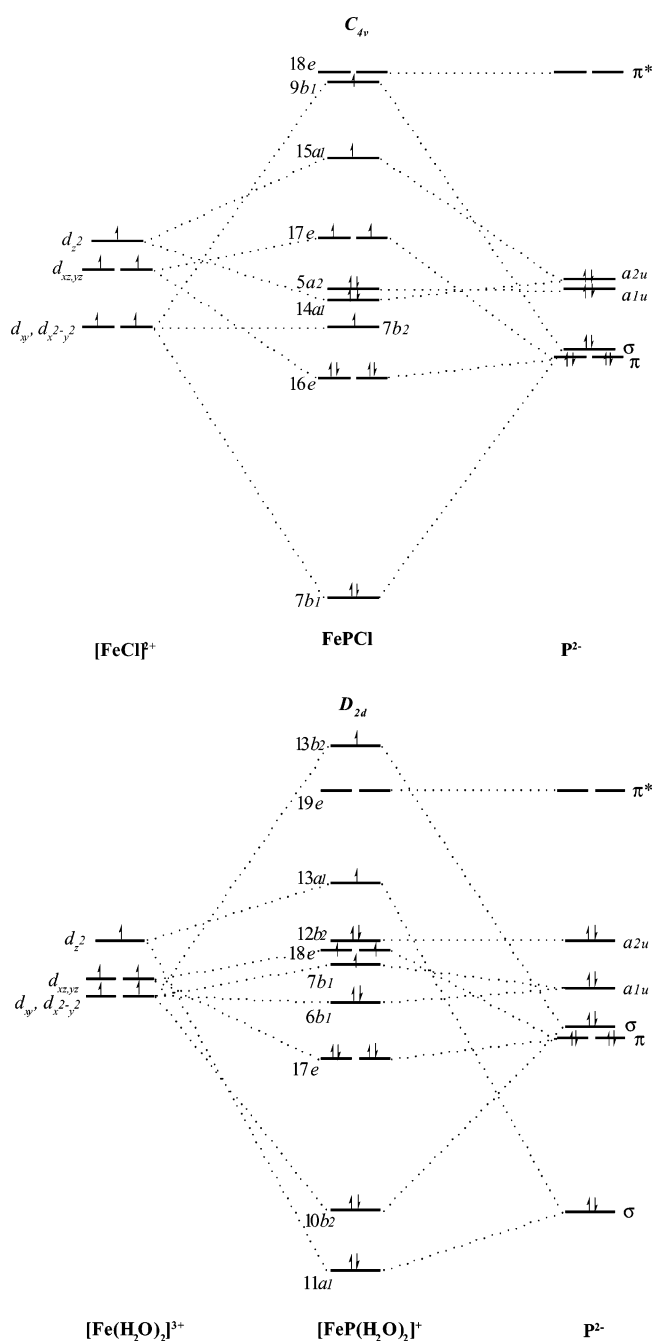
Figure 5. Molecular orbital energy level correlation diagrams for FePCl and [FeP(H₂O)₂]⁺ complexes.

interactions.[20] There are no metal orbitals that have a₂ symmetry in either the FePCl or [FeP(H₂O)₂]⁺ complex. Rather, the stabilization arises from the relaxation of the occupied a₂ orbitals of the porphyrin caused by the electrostatic attraction of the metal. The positive charge of the metal fragment polarizes the electronic charge distribution of the porphyrin fragment. It is very dangerous to compare the absolute numbers of the energy decomposition analysis of two systems when the charges of the chosen fragments in the two systems are different, that is, FeCl²⁺/P²⁻ versus Fe(H₂O)₂³⁺/P²⁻. The electrostatic stabilization of the a₂ orbitals is somewhat larger for [FeP(H₂O)₂]⁺, which must be ascribed to the tripositive cation [Fe(H₂O)₂]³⁺. Similar contributions should be recognized for all orbital interaction

terms in the positively charged system, and this indirect electrostatic effect is responsible for part of the observed larger $\Delta E(d_{z^2})$ in [FeP(H₂O)₂]⁺. On the basis of the orbital overlaps related to $d_{x^2-y^2}$ and $d_{xz,yz}$ from Table 7 and $\Delta E(a_2)$ in FePCl and [FeP(H₂O)₂]⁺, a rough approximation of this indirect electrostatic effect has been estimated to be ∼7−16%. The lower limit of $\Delta E(d_{z^2})$ in FePCl will then be 151 kcal/mol, which is still 41 kcal/mol higher than the 110 kcal/mol obtained from the calculation. This may be ascribed to different spatial distribution of the electron density that contributes to σ-type and π-type bonding interactions (vide supra).

As noted earlier, the total orbital interaction energy in e symmetry is the sum of forward- and back-bonding components, and it is not possible to deconvolute the contribution of the two components simply on the basis of symmetry. It is, however, possible to determine the contribution of the Fe → P π* back-bonding indirectly by removing the vacant π* orbitals of the porphyrin macrocycle from the valence space.[19] Although the difference between the two interaction energies (before and after removal of the π* orbitals) provides a reasonable estimation of the contribution of Fe → P π* back-bonding, the residual interaction energy in e symmetry is only a rough approximation to P → Fe π forward-bonding due to the contribution from the indirect electrostatic effect. The possibility to estimate this P → Fe π forward-bonding interaction the other way around, through removal of the vacant metal dπ orbitals, is limited by the d⁵ high-spin nature of the metal fragment. The change in energy decomposition components after removal of the π* is also shown in Table 8. It is evident that removal of the π* orbital has ∼10% effect on the bonding interaction of e symmetry. Consistent with the molecular orbital representations (Figure 3), the majority of the orbital interaction energy in e symmetry clearly arises through P → Fe π forward bonding for both five- and six-coordinate complexes.

All of the bonding interactions are summarized semiquantitatively in the molecular orbital energy level correlation diagrams as shown in Figure 5 for both FePCl and [FeP(H₂O)₂]⁺ complexes. This figure takes into account the energy difference between fragment orbitals and the strength of orbital interactions and should be the most friendly way to demonstrate the data.

Conclusions

Symmetry-controlled bonding interactions between iron and porphyrin macrocycle of five- and six-coordinate high-spin iron-(III)−porphyrin complexes are analyzed within the framework of approximate density functional theory in this report. Working in combination, spin-restricted and -unrestricted calculations demonstrate that, whereas only the latter (with consideration of exchange correlation) will result in the spin density distribution on the molecule, the former gives a clear average view of the molecular orbital representation. Qualitatively, the relative extent of the iron−porphyrin interactions can be evaluated through spin population and orbital contribution analyses. Deconvolution of the gross spin populations into the components of σ and π symmetry offers a unique chance to look into the mechanism of spin delocalization and the source of the observed paramagnetic shift. Quantitatively, the bond strengths corresponding to different symmetry representations can be approximated by the use of the energy decomposition scheme. Further deconvolution of the orbital interaction energies into

the component of P → Fe π donation and Fe → P π^* back-bonding is approximated through the possibility of removing the vacant π^* orbitals of the porphyrin from the valence space. In contrast to previous suggestions, there are only limited Fe → P π^* back-bonding interactions in high-spin iron(III)−porphyrin complexes. It is the symmetry-allowed bonding interaction between d_{z^2} and a_{2u} orbitals that is responsible for the positive π spin densities at the *meso*-carbons of five-coordinate iron(III)−porphyrin complexes. Both five- and six-coordinate complexes show significant P → Fe π donation, which is further enhanced by the movement of the metal toward the in-plane position for six-coordinate complexes. These bonding characteristics correlate very well with the NMR data reported experimentally for these paramagnetic complexes. Further quantitative correlation between the spin population and the contact shift of paramagnetic molecules can be facilitated by the evaluation of the unpaired electron spin density on the nuclei, which will be the subject of our next paper.[39]

The possibility of a bonding interaction between d_{z^2} and a_{2u} orbitals has always been neglected due to the general recognition that d_{z^2} is a σ-type orbital, whereas a_{2u} is of π type. However, for five-coordinate complexes with the metal sitting out-of-plane toward the axial ligand, d_{z^2} can actually behave as a π-type orbital with respect to the porphyrin macrocycle. From this point of view, the bonding interaction between d_{z^2} and a_{2u} orbitals would decrease as the out-of-plane displacement of metal decreases. This is consistent with the fact that *meso*-H shifts downfield when the metal moves back toward the center, as the contribution of $S = {}^3/_2$ increases.[1] Further support from theoretical calculations was clearly indicated by the decreased positive spin densities at *meso*-C positions for admixed-spin complexes.

Within the five d orbitals, d_{z^2} is the one most accessible to the σ donation interaction from the axial ligands. The unique bonding interaction between d_{z^2} and a_{2u} orbitals in five-coordinate metalloporphyrin complexes provides a novel symmetry-controlled mechanism for spin transfer between the axial ligand σ system and the porphyrin π system. On the other hand, this suggests the possibility of axial ligand-controlled spin coupling between d_{z^2} and a_{2u} porphyrin π cation radicals, which has been established in the $[Co^{II}(OETPP)^{+\cdot}X]$ (X = Cl, Br, I) system.[42] The biological implications of this spin transfer pathway are being investigated.

Supporting Information Available: Table of contact shifts and Fermi contact spin densities and the corresponding correlation diagram for Fe^{III}PCl (P = TPP, OEP). This material is available free of charge via the Internet at http://pubs.acs.org.

JA021344N

(42) Cheng, R.-J.; Chen, P.-Y.; Peng, S.-M. In preparation.
(43) Behere, D. V.; Birdy, R.; Mitra, S. *Inorg. Chem.* **1982**, *21*, 386−390.
(44) Boersma, A. D.; Goff, H. M. *Inorg. Chem.* **1982**, *21*, 581−586.
(45) Phillippi, M. A.; Baenziger, N.; Goff, H. M. *Inorg. Chem.* **1981**, *20*, 3904−3911.
(46) Walker, F. A.; La Mar, G. N. *Ann. N. Y. Acad. Sci.* **1973**, *206*, 328−348.
(47) Toney, G. E.; Gold, A.; Savrin, J.; Terhaar, L. W.; Sangaiah, R.; Hatfield, W. E. *Inorg. Chem.* **1984**, *23*, 4350−4352.